Causally-motivated Shortcut Removal Using Auxiliary Labels

Maggie Makar* CSAIL, MIT mmakar@mit.edu Ben Packer Google Research bpacker@google.com Dan Moldovan Google Research mdan@google.com

Davis Blalock MosaicML davis@mosaicml.com

Yoni Halpern Google Research yhalpern@google.com Alexander D'Amour Google Research alexdamour@google.com

Abstract

Robustness to certain forms of distribution shift is a key concern in many ML applications. Often, robustness can be formulated as enforcing invariances to particular interventions on the data generating process. Here, we study a flexible, causally-motivated approach to enforcing such invariances, paying special attention to shortcut learning, where a robust predictor can achieve optimal *iid* generalization in principle, but instead it relies on spurious correlations or shortcuts in practice. Our approach uses auxiliary labels, typically available at training time, to enforce conditional independences between the latent factors that determine these labels. We show both theoretically and empirically that causally-motivated regularization schemes (a) lead to more robust estimators that generalize well under distribution shift, and (b) have better finite sample efficiency compared to usual regularization schemes, even in the absence of distribution shifts. Our analysis highlights important theoretical properties of training techniques commonly used in causal inference, fairness, and disentanglement literature.

1 Introduction

Despite their immense success, predictors constructed from deep neural networks (DNNs) have been shown to lack robustness under distribution shift [Beery et al., 2018, Ilyas et al., 2019, Azulay and Weiss, 2018, Geirhos et al., 2018], especially naturally occurring distribution shifts [Taori et al., 2020]. One particular mechanism for this brittleness is *shortcut learning* [Geirhos et al., 2020]. Shortcut learning occurs when a predictor relies on input features that are easy to represent (i.e., shortcuts) and are predictive of the outcome in the training data, but do not remain predictive when the distribution of inputs changes.

^{*}Part of this work was completed while MM was an intern at Google Research

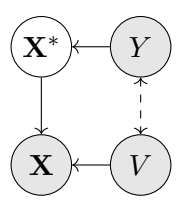


Figure 1: Causal DAG of the setting in this paper. The main label Y and auxiliary label V generate observed input X, but Y only affects X through the sufficient statistic X^* .

For example, a DNN trained for image classification could exploit correlations between the foreground object and background of images in the training distribution, and use a representation of the background as a shortcut to predict the foreground object [Beery et al., 2018, Sagawa et al., 2019]. This holds even if the foreground object alone is sufficient to achieve optimal predictive performance [Nagarajan et al., 2020, Sagawa et al., 2020a].

Throughout the paper, we use the example of classifying the foreground object as land or water bird, adapted from [Sagawa et al., 2019]. The two classes are visually distinct but the majority of the former often appear on land backgrounds, and the latter on water backgrounds. DNNs that exploit shortcuts could achieve strong performance on unseen instances from the training distribution, but would fail if the foreground object and background were correlated differently in the test distribution (e.g., if water birds appeared on land backgrounds). More generally, models that rely on shortcuts are vulnerable to shifts in distribution induced by intervening on factors of variation that are correlated—but not causally related—with the main label in the training distribution.

In this paper, we consider the problem of learning a performant predictor whose risk is invariant to interventions that change the correlations between irrelevant factors and the main label. Ideally, such a predictor would rely exclusively on input features that are invariant to irrelevant factors. However, identifying such invariant input features in the standard supervised learning setup is difficult, for the same reason that shortcut learning is successful: in learning setups where there are many distinct ways to construct predictors that perform well on held-out data (i.e., when the learning problem is underspecified [D'Amour et al., 2020]), the influence of correlated factors is difficult to disentangle without additional supervision [Locatello et al., 2019].

For this reason, we focus on a modified setting where we are also given an auxiliary label that gives information about the irrelevant factor. Such labels often appear in the form of metadata associated with training data—for example, labels of the background—but are often not available at test time. In this setting, we propose an approach that exploits this auxiliary label to construct a predictor whose risk is approximately invariant across a well-defined family of test-distributions. Our method makes use of two tools from causal inference in combination: (1) weighting the training data to mimic an idealized population, and (2) enforcing an independence implied by the causal Directed Acyclic Graph (DAG) in that idealized population. While each of these approaches has been applied separately, we show here through both theoretical arguments and empirical analysis that these methods

are particularly effective when applied together.

Our methodological contributions can be summarized as follows: (1) We suggest an approach to discourage shortcut learning using auxiliary labels, and specify a set of distribution shifts across which a robust model is risk-invariant. (2) We give a theoretical justification to our approach, highlighting that in some scenarios it yields models that have a lower generalization error than typical regularization schemes. We also show that our approach is robust to a set of distribution shifts. (3) We empirically validate our theoretical findings using a semi-simulated benchmark, showing our approach has favorable in- and out-of-distribution generalization properties. (4) We compare against baselines that ablate each part of our approach to show that their combination yields more performant, stable training.

The remainder of the paper is organized as follows. In section 2, we formally introduce our objective. We also discuss important properties of the unconfounded distribution, where the main label and the auxiliary label are independent. In section 3, we present our main approach, and briefly state the main claims that guide the design of our approach. We revisit these claims in section 4 with a greater detail, giving theoretical justification for each. We present our empirical analysis in section 5, and conclude in section 7.

2 Preliminaries

2.1 Setup

We consider a supervised learning setup where the task is to construct a predictor $f(\mathbf{X})$ parameterized by weights \mathbf{w} that predicts a label Y (e.g., foreground object) from an input \mathbf{X} (e.g., image). In addition, we have an auxiliary label V (e.g., background label) available only at training time that labels a factor of variation along which we hope the model will exhibit some invariance (e.g., background type). Throughout, we will use capital letters to denote variables, and small letters to denote their value. Our training data consist of tuples $\mathcal{D} = \{(\mathbf{x}_i, y_i, v_i)\}_{i=1}^n$ drawn from a source training distribution P_s . We restrict our focus to the case where Y and V are binary and f is a classifier. Specifically, we will consider functions f of the form $f = h(\phi(\mathbf{x}))$, where ϕ is a representation mapping and h is the final classifier.

Assumptions. We assume that P_s has a generative structure shown in Figure 1, in which the inputs X are generated by the labels (Y, V). We assume that the labels Y and V are are correlated, but not causally related; that is, an intervention on V does not imply a change in the distribution of Y, and vice versa. Such correlation often arises through the influence of an unobserved third variable such as the environment from which the data is collected. We represent this in Figure 1 with the dashed bidirectional arrow.

In addition, we assume that there is a sufficient statistic X^* such that Y only affects X

through \mathbf{X}^* , and \mathbf{X}^* can be fully recovered from \mathbf{X} via the function $\mathbf{X}^* := e(\mathbf{X})$. However, we assume that the sufficient reduction $e(\mathbf{X})$ is unknown, so we denote \mathbf{X}^* as unobserved in Figure 1.

We also make an overlap assumption on the source distribution, P_s . Specifically we assume that $P_s(V)P_s(Y) \ll P_s(V,Y)$ with $0 < P_s(V)P_s(Y) < 1$.

2.2 Risk Invariance and Shortcut Learning

We define the generalization risk of a function f on a distribution P as $R_P = \mathbb{E}_{X,Y \sim P}[\ell(f(X),Y)]$, where ℓ is the logistic loss.

We focus on obtaining an optimal risk invariant predictor, with the property that the risk of the predictor is invariant across a family of target distributions \mathcal{P} that can be obtained from P_s by interventions on the causal model in Figure 1. Specifically, we consider interventions on the confounding relationship between Y and V that keep the marginal distribution of Y constant. Each distribution in this family can be obtained by replacing the source conditional distribution $P_s(V \mid Y)$ with a target conditional distribution $P_t(V \mid Y)$:

$$\mathcal{P} := \{ P_s(\mathbf{X} \mid \mathbf{X}^*, V) P_s(\mathbf{X}^* \mid Y) P_s(Y) P_t(V \mid Y) \}, \tag{1}$$

This family allows the dependence between Y and V to change arbitrarily.

Given the family \mathcal{P} , we define the set of risk invariant predictors to be all predictors that have the same risk for all $P_t \in \mathcal{P}$,

$$\mathcal{F}_{\text{rinv}} = \{ f : R_{P_t}(f) = R_{P_t'}(f) \quad \forall P_t, P_t' \in \mathcal{P} \}$$

and an optimal risk-invariant predictor $f_{\rm rinv}$ to have the property

$$f_{\text{rinv}} \in \arg\min_{f \in \mathcal{F}_{\text{rinv}}} R_{P_t}(f) \quad \forall P_t \in \mathcal{P}.$$

Any predictor that does not rely on the "shortcut" factor labeled by V will necessarily be risk invariant; thus, it is a natural property to test for and enforce for shortcut removal. Risk invariance is also independently appealing because guarantees about the performance of the predictor f_{rinv} derived under one distribution can be adapted to other distributions in \mathcal{P} .

2.3 The Unconfounded Distribution P°

Within the family of distributions \mathcal{P} , we pay special attention to the unconfounded distribution $P^{\circ} \in \mathcal{P}$ where $P^{\circ}(V \mid Y) := P_s(V)$. Under P° , $Y \perp V$ and the dashed bidirectional arrow in Figure 1 can be dropped. Both our methodological approach and theoretical analysis revolve around mapping the problem of learning a risk invariant predictor under P_s to the problem of learning an optimal predictor under P° .

 P° has two useful properties that are revealed by the DAG in Figure 1: (1) under the unconfounded distribution P° , the optimal predictor (with some abuse of notation) would take the form $f(\mathbf{X}^*)$, and (2) for any predictor of the form $f(\mathbf{X}^*)$, the joint distribution $P(f(\mathbf{X}^*), Y)$ (and thus the risk) is invariant across the family \mathcal{P} . Together, these imply that the optimal risk-invariant predictor $f_{\text{rinv}}(\mathbf{X}^*)$ is the optimal predictor under P° . We state this formally in the following proposition.

Proposition 1. Under P° , the Bayes optimal predictor is (i) only a function of \mathbf{X}^{*} , and (ii) an optimal risk-invariant predictor f_{rinv} with respect to \mathcal{P} .

The proof for this proposition, and all others presented in this paper, are shown in the appendix.

Proposition 1 motivates our approach to design an objective that enables efficient estimation of the optimal predictor under P° , even when the training data \mathcal{D} are drawn from $P_s \neq P^{\circ}$.

3 Approach

Here, we describe our approach to learning an optimal risk-invariant predictor $f_{\text{rinv}}(\mathbf{X})$ from training data $\mathcal{D} \sim P_s$. Our strategy follows the schematic $P_s \to P^{\circ} \to P_t$: to learn a risk invariant predictor under P_s , we map the learning problem to P° , then learn a predictor under P° that will generalize well to any P_t in \mathcal{P} . The $P_s \to P^{\circ}$ step is achieved by importance weighting, which is relatively familiar to a wider audience. So we focus first on our proposed regularization scheme that aids with the $P^{\circ} \to P_t$ step.

Regularization under P° . Our main innovation is a regularization scheme that leverages knowledge of the causal DAG to efficiently learn a classifier under P° . Specifically, we use two facts that hold under P° : (1) $V \perp \mathbf{X}^{*}$, and (2) the optimal predictor is only a function of \mathbf{X}^{*} (Proposition 1). As we show in Section 4, this regularizer can help to reduce the sample complexity of learning without inducing bias, and directly penalizes the gap between the risk under P° and P_{t} .

Based on these facts, we specify a regularizer for $f = h(\phi(\mathbf{X}))$ that encourages $\phi(\mathbf{X}) \perp V$. We do this by penalizing a distributional discrepancy between conditional distributions of the representation $P^{\circ}(\phi(\mathbf{X}) \mid V = 0)$ and $P^{\circ}(\phi(\mathbf{X}) \mid V = 1)$ that would be identical under independence. Although any number of estimable distributional discrepancy metrics could be used, here we choose to use the Maximum Mean Discrepancy (MMD), defined as follows:

Definition 1. Let Z, and Z', be two arbitrary variables with $Z, Z' \in \mathcal{Z}$, and let their corresponding distributions be P_Z and $P_{Z'}$. And let Ω be a class of functions $\omega : \mathcal{Z} \to \mathbb{R}$,

$$\mathrm{MMD}(\Omega, P_Z, P_{Z'}) = \sup_{\omega \in \Omega} \bigl(\mathbb{E}_{P_Z} \omega(Z) - \mathbb{E}_{P_{Z'}} \omega(Z') \bigr).$$

When Ω is set to be a general reproducing kernel Hilbert space (RKHS), the MMD defines a metric on probability distributions, and is equal to zero if and only if $P_Z = P_{Z'}$. Throughout,

we will assume that our predictor f and our loss ℓ are contained in Ω , and in practice choose Ω to be the RKHS induced by the radial basis function (RBF) kernel. We will use the shorthand $\text{MMD}(P_Z, P_{Z'})$ to denote $\text{MMD}(\Omega, P_Z, P_{Z'})$. See Gretton et al. [2012] for a review of MMD and its empirical estimators.

Weighting to Recover P° . When the training data is drawn from some $P_s \neq P^{\circ}$, we weight the data to obtain empirical risk and MMD expressions that are unbiased estimates of the expressions we would obtain if $\mathcal{D} \sim P^{\circ}$, and proceed as before. In particular, we define weights

$$u(y,v) = \frac{P_s(Y=y)P_s(V=v)}{P_s(Y=y,V=v)},$$
(2)

such that for each example, $u_i := u(y_i, v_i)$. We use \tilde{u}_i to denote u_i after normalization such that $\sum_i \tilde{u}_i = 1$. For any distribution P_s , these are importance weights that map expectations under P_s to expectations under P° . In the appendix, we show that the reweighted risk is an unbiased estimator of the risk under P° , i.e., that $\mathbb{E}_{P_s}\left[\hat{R}^{\mathbf{u}}_{P_s}(f)\right] = R_{P^{\circ}}(f)$, where $\hat{R}^{\mathbf{u}}_{P_s}(f) = \sum_i \tilde{u}_i \ell(f(\mathbf{x}_i), y_i)$, and $R_{P^{\circ}}(f) = \mathbb{E}_{\mathbf{X}, Y \sim P^{\circ}}\left[\ell(f(\mathbf{X}), Y)\right]$.

Method Putting the different components of our approach together gives us a final objective to optimize: let ϕ_v denote $\{\phi(\mathbf{x}_i)\}_{i:v_i=v}$, and $\phi_v^{\mathbf{u}}$ denote its re-weighted analogue, and let u_i be as in equation 2. For $\mathcal{D} \sim P_s$, and some $\alpha > 0$, the main objective to minimize is:

$$h^*, \phi^* = \underset{h, \phi}{\operatorname{argmin}} \sum_{i} u_i \ell(h(\phi(\mathbf{x}_i)), y_i) + \alpha \cdot \widehat{\text{MMD}}^2(P_{\phi_0^{\mathbf{u}}}, P_{\phi_1^{\mathbf{u}}}).$$
 (3)

To estimate $\widehat{\text{MMD}}^2$, we use a weighted version of the V-statistic estimator presented in Gretton et al. [2012]. Specifically, we compute:

$$\widehat{\text{MMD}}^2 = \sum_{i,j:v_i,v_j=0} \overline{u}_i \overline{u}_j k_{\gamma}(\phi_i, \phi_j) + \sum_{i,j:v_i,v_j=1} \overline{u}_i \overline{u}_j k_{\gamma}(\phi_i, \phi_j) - 2 \sum_{i,j:v_i=0,v_j=1} \overline{u}_i \overline{u}_j k_{\gamma}(\phi_i, \phi_j),$$

where $k_{\gamma}(x, x')$ is the radial basis function, with bandwidth γ , and the weights \overline{u}_i are a normalized version of u_i such that $\sum_{i,j:v_i,v_j=0} \overline{u}_i \overline{u}_j = \sum_{i,j:v_i,v_j=1} \overline{u}_i \overline{u}_j = \sum_{i,j:v_i=0,v_j=1} \overline{u}_i \overline{u}_j = 1$

Cross-validation The objective function in (3) depends on two hyperparameters. The first is the cost of the MMD penalty α , and the second is γ , the kernel bandwidth necessary to compute the MMD term. Unlike the usual regularization schemes, the MMD-regularization term also depends on the distribution of the data, and is subject to errors caused by finite samples. In other words, it is possible to overfit this objective such that the MMD on the training data is 0 but it remains large on a validation set. For this reason, we follow a two-step cross-validation procedure. In the first step, we calculate the weighted MMD

on each of the K validation folds. We then exclude all models that achieve a weighted MMD that is statistically significantly different from zero. This gives us a subset of the function candidates that encode the desired invariances. In the second step, we pick the best performing model out of this subset of candidate functions.

4 Theory

In this section, we analyze our approach in some important special cases to show how it encourages efficient learning of a risk-invariant predictor on \mathcal{P} . We focus on the generalization gap of a predictor learned under a source distribution P_s when evaluated on any target distribution P_t , that is, the difference between the target risk R_{P_t} and the weighted empirical risk $\hat{R}_{P_s}^{\mathbf{u}} = \sum_i \tilde{u}_i \ell(f(\mathbf{x}_i), y_i)$ for a learned function f. In keeping with our schematic $P_s \to P^\circ \to P_t$ (described in Section 3), we decompose this gap into a term about generalizing from P_s to P° , and a term about generalizing from P° to P_t :

$$R_{Pt}(f) - \hat{R}_{Ps}^{\mathbf{u}}(f) = \underbrace{R_{Pt}(f) - R_{P^{\circ}}(f)}_{\text{Structural risk gap } (P^{\circ} \to P_t)} + \underbrace{R_{P^{\circ}}(f) - \hat{R}_{Ps}^{\mathbf{u}}(f)}_{\text{Finite-sample gap } (P_s \to P^{\circ})}. \tag{4}$$

We show that constraints on the MMD between the learned representation distributions $P^{\circ}(\phi(\mathbf{X}) \mid V = v)$ for $v \in \{0,1\}$, which we denote $\mathrm{MMD}(P_{\phi_0}^{\circ}, P_{\phi_1}^{\circ})$, can translate to constrains on both of these gaps. We treat the structural risk gap first, but spend the bulk of our effort on the finite-sample gap in the linear case.

4.1 Bounding the structural risk gap

We begin by bounding the structural risk gap, $R_{Pt}(f) - R_{P^{\circ}}(f)$, which characterizes how the risk for a given function f learned on data from P° is related to the risk on any target distribution $P_t \in \mathcal{P}$. Here, we show that a bound on $\text{MMD}(P_{\phi_0}^{\circ}, P_{\phi_1}^{\circ})$ translates directly to a bound on the structural risk gap in the representable case, when Y can be written as a function of the representation $\phi(\mathbf{X})$.

Proposition 2. Suppose that $f = h(\phi(\mathbf{X}))$ is a predictor that satisfies $\mathrm{MMD}(P_{\phi_0}^{\circ}, P_{\phi_1}^{\circ}) \leq \tau$. Suppose that y is ϕ -representable, i.e., that there exists $g(\phi(\mathbf{x})) = y$, and that $g(\phi)\ell(\phi) \in \Omega$. Then

$$R_{Pt}(f) < R_{P^{\circ}}(f) + 2\tau.$$

Proposition 2 motivates the MMD penalty. The MMD penalty directly encourages small values of τ ; this regularizes the solution toward a predictor that has similar risks on P_t , and P° . This in turn means that the first term in equation 4 is small, leading to low generalization error of our proposed weighted estimator.

4.2 Bounding the finite-sample gap

We now analyze how the MMD regularizer constrains the finite-sample gap, $R_{P^{\circ}}(f) - \hat{R}_{P_s}^{\mathbf{u}}(f)$. This gap characterizes how the weighted empirical risk, which is minimized during training on data drawn from P_s , translates to risk on the unconfounded distribution P° . Here, we consider the special case of linear models, where ϕ is a linear mapping, i.e., $\phi(\mathbf{x}) = \mathbf{w}^{\top}\mathbf{x}$, and h is the sigmoid, i.e., $h(x) = \sigma(x) = 1/(1 + \exp(-x))$. Our analysis establishes some key insights about how the MMD regularizer constrains the learning problem, and when we expect it to provide significant efficiency gains. Extensions of our theoretical analysis to more complex neural networks are possible (e.g., through approaches studied in Golowich et al. [2018]).

Controlling the complexity. There are two issues to consider in bounding this gap. The first is the fundamental generalization gap that we would face if we were learning f directly on "ideal" samples from P° , and the second is the additional variability incurred by importance weighting to translate the learning problem to P° to P_s , from which we actually observe samples. Importantly, regularization affects both the "ideal" and weighted learning problems in the same way, by restricting the complexity of the function class \mathcal{F} . Thus we focus on the Rademacher complexity of the function class obtained by constraining $\text{MMD}(P_{\phi_0}^{\circ}, P_{\phi_1}^{\circ})$.

Definition 2. Let $\epsilon = {\{\epsilon_i\}_{i=1}^n}$ denote a vector of independent random variables drawn from the Rademacher distribution, i.e., uniform on $\{-1,1\}$. For a function family \mathcal{F} , and $\mathcal{D} \sim P$, the Rademacher complexity for a sample of size n is defined as:

$$\mathfrak{R}(\mathcal{F}) = \mathbb{E}_{\mathcal{D}} \mathbb{E}_{\epsilon} \left[\sup_{f \in \mathcal{F}} \frac{1}{n} \sum_{i=1}^{n} \epsilon_{i} f(\mathbf{x}_{i}) \right].$$

In the ideal case, where $P_s = P^{\circ}$, the Rademacher complexity translates directly to a bound on the finite-sample or generalization gap. Specifically, the generalization gap increases as $\Re(\mathcal{F})$ increases (see [Mohri et al., 2018]). For the case where $P_s \neq P^{\circ}$, and weighting is necessary, we can obtain a bound that is similarly monotonic in $\Re(\mathcal{F})$ using the technique of Cortes et al. [2010]. Due to space limitations, we focus on analyzing the Rademacher complexity of the MMD regularized space in the main text and present the full generalization error bounds for both cases in the appendix, section D.1.

Comparison with L2 Regularization To analyze how constraints on $\text{MMD}(P_{\phi_0}^{\circ}, P_{\phi_1}^{\circ})$ affect Rademacher complexity, we study how the addition of an MMD constraint shrinks a standard L2-regularized function class. Define the two function classes:

$$\mathcal{F}_{L_2} := \{ f : \mathbf{x} \mapsto \sigma(\mathbf{w}^\top \mathbf{x}), \|\mathbf{w}\|_2 \le A \},$$
 (5)

$$\mathcal{F}_{L_2,\text{MMD}} := \{ f : \mathbf{x} \mapsto \sigma(\mathbf{w}^{\top} \mathbf{x}), \|\mathbf{w}\|_2 \le A, \text{ MMD}(P_{\phi_0}^{\circ}, P_{\phi_1}^{\circ}) \le \tau \}.$$
 (6)

Before analyzing the precise reduction in complexity in moving from \mathcal{F}_{L_2} to $\mathcal{F}_{L_2,\text{MMD}}$, we note that this reduction is a "free lunch": because we know that the MMD constraint is compatible with the true independence structure of P° , this reduction does not introduce bias. We state this formally in the following proposition.

Proposition 3. For $\mathcal{D} \sim P^{\circ}$, and for any for \mathcal{F}_{L_2} such that $f_{rinv} \in \mathcal{F}_{L_2}$, there exists $\mathcal{F}_{\text{MMD},L_2} \subseteq \mathcal{F}_{L_2}$ such that $f_{rinv} \in \mathcal{F}_{\text{MMD},L_2}$. And the smallest $\mathcal{F}_{\text{MMD},L_2}$ such that $f_{rinv} \in \mathcal{F}_{\text{MMD},L_2}$ has MMD = 0.

To study the reduction in complexity more explicitly, we construct comparable Rademacher complexity upper bounds for \mathcal{F}_{L_2} and $\mathcal{F}_{L_2,\text{MMD}}$. Here, we focus on a specific implication of the MMD constraint in the case where ϕ is a linear mapping. In this setting, the constraint restricts the projection of the predictor weights \mathbf{w} onto the vector that distinguishes the conditional means: $\Delta := \boldsymbol{\mu}_0 - \boldsymbol{\mu}_1$, where $\boldsymbol{\mu}_v := \mathbb{E}_{\mathbf{x} \sim P^\circ}[\mathbf{X} \mid V = v]$. Δ is the average change in \mathbf{X} caused by intervening to change the V under P° . Define the projection matrix $\Pi := \Delta(\Delta^\top \Delta)^{-1}\Delta^\top = \|\Delta\|_2^{-2}\Delta\Delta^\top$, which projects any vector onto Δ . We then define $\mathbf{w}_\perp := \Pi \mathbf{w}$ as the projection of \mathbf{w} onto the mean distinguishing vector Δ , which can be thought of as the "bad" or "irrelevant" dimension of \mathbf{X} .

We can directly relate $\|\mathbf{w}_{\perp}\|$ to the MMD constraint, in the following proposition.

Proposition 4. Let $f(\mathbf{x}) = \sigma(\phi(\mathbf{x})) = \sigma(\mathbf{w}^{\top}\mathbf{x})$ be a function contained in $\mathcal{F}_{L_2,\text{MMD}}$. Then,

$$\|\mathbf{w}_{\perp}\| \le \frac{\tau}{\|\Delta\|}.$$

Intuitively, proposition 4 says that the MMD constraint limits the effect of the irrelevant components of \mathbf{w} proportionally to τ . In the image classification example, where V labels the background type, this means that the parts of \mathbf{w} that can discriminate between images with different background types is directly constrained by τ .

Using this fact, we derive comparable bounds on the Rademacher complexity of the two function classes by splitting f in terms of how the observed features \mathbf{x} align with the mean difference vector Δ . Here, we let $\mathbf{x}_{\perp} := \Pi \mathbf{x}$ be the component of \mathbf{x} that is parallel to the mean discrepancy i.e., parallel to the "irrelevant component," and hence perpendicular to the relevant components. We let $\mathbf{x}_{\parallel} := (I - \Pi)\mathbf{x}$ be the orthogonal component to the irrelevant components (i.e., the "relevant component").

Proposition 5. Let $\mathbf{x}_{\perp} := \Pi \mathbf{x}$, $\mathbf{x}_{\parallel} := (I - \Pi) \mathbf{x}$. For training data $\mathcal{D} = \{(\mathbf{x}_i, y_i, v_i)\}_{i=1}^n$, $\mathcal{D} \sim P^{\circ}$, $\sup_{\mathbf{x}_{\perp}} \|\mathbf{x}_{\perp}\|_2 \leq B_{\perp}$, $\sup_{\mathbf{x}_{\parallel}} \|\mathbf{x}_{\parallel}\|_2 \leq B_{\parallel}$, then

$$\Re(\mathcal{F}_{L_2}) \leq \frac{A\sqrt{B_{\parallel}^2 + B_{\perp}^2}}{\sqrt{n}},$$

$$and$$

$$\Re(\mathcal{F}_{\text{MMD},L_2}) \leq \frac{A \cdot B_{\parallel} + \tau \frac{B_{\perp}}{\parallel \Delta \parallel}}{\sqrt{n}}.$$

The proof applies a standard Rademacher complexity bound for the L_2 class, and applies a more conservative strategy for $\mathcal{F}_{\text{MMD},L_2}$ by separately bounding the worst-case terms involving \mathbf{x}_{\perp} and \mathbf{x}_{\parallel} . Nonetheless, comparing these bounds is instructive. In particular, the upper bound on $\mathfrak{R}(\mathcal{F}_{\text{MMD},L_2})$ is smaller than that of $\mathfrak{R}(\mathcal{F}_{L_2})$ whenever τ satisfies:

$$0 \le \tau < A \left[\sqrt{B_{\parallel}^2 + B_{\perp}^2} - B_{\parallel} \right] \frac{\|\Delta\|}{B_{\perp}}. \tag{7}$$

The key part of this expression is the ratio $\|\Delta\|/B_{\perp}$, which can be understood as a characterization of how much of the variation in \mathbf{x}_{\perp} comes from the mean shift in \mathbf{x} induced by v. In particular, when the variation caused by mean shift is large, we expect even weak MMD regularization to yield better generalization than L_2 regularization alone, and we expect this effect to be even stronger when variation in the mean shift direction is large relative to variation in orthogonal directions. This occurs in cases where V controls features that are highly salient in the input \mathbf{x} . For example, in object recognition using images, if V denotes the background type, we expect $\|\Delta\|/B_{\perp}$ to be large if the background features are very different between V=0 and V=1, but relatively consistent within values of V. Further, if the background accounts for the majority of pixels in each image, we expect $B_{\perp} \gg B_{\parallel}$, resulting in an even stronger regularizing effect from the MMD penalty.

In the appendix, we show why naively enforcing the MMD penalty without reweighting when $P_s \neq P^{\circ}$ can introduce biased estimation. These findings have implications that extend beyond shortcut learning, e.g., fairness and causality where the MMD penalty is frequently used.

5 Experiments

In this section, we empirically demonstrate that our approach can mitigate shortcut learning. Specifically, in a setting where models that exploit shortcuts show highly variable risk across test sets, our method produces predictors that are closer to risk invariant. We also show that, as our theory suggests, our approach leads to more efficient estimation under the "ideal" distribution even in the absence of correlated sampling or distribution shift.

Data. We conduct all of our experiments using the semi-synthetic "waterbirds" setup presented in Sagawa et al. [2019], which allows control of the correlation between Y, the type of bird in an image, and V, the type of background. Specifically, we construct a dataset that combines images of water birds (Gulls) and land birds (Warblers) extracted from the Caltech-UCSD Birds-200-2011 (CUB) dataset [Wah et al., 2011] with water and land background extracted from the Places dataset [Zhou et al., 2017].

We found that the original background images frequently contain landscapes that are difficult to distinguish (e.g., water backgrounds with very small water bodies that mostly reflect the surrounding trees). Instead, we pick 300 "clean" images for each of the land and water backgrounds. Using those clean images, we generate 10,000 land backgrounds,

and 9,000 water backgrounds by applying random transformations (rotation, zoom, dark-ening/brightening) to the selected images. In the appendix, we present the results on the original backgrounds.

Additional details about data generation, and hyperparameter selection are included in the appendix.

Settings. We examine how a model trained under a specific distribution P_s generalizes to various test distributions $P_t \in \mathcal{P}$. We consider two different cases for P_s . In the first, we consider training under ideal conditions, where $P_s = P^{\circ}$. This setting tests the implications of proposition 5, which suggests that our approach improves sample effection even under uncorrelated sampling. This is one of the main mechanisms by which our approach is meant to reduce the risk gap in (4). In the second setting, the training data is sampled from a P_s where the auxiliary label and the main label are correlated, i.e., $V \not\perp V$.

For the first setting, we generate the training data from the ideal distribution P° , with $P^{\circ}(Y|V=1) = P^{\circ}(Y|V=0) = 0.5$. In the second setting, we generate the data such that P(Y=1|V=1) = P(Y=0|V=0) = 0.9, representing a scenario where the majority of water birds are on water backgrounds and the majority of land birds are on land backgrounds. For both settings, we introduce noise by randomly flipping 1% of each of the labels. We generate a number of held-out test sets, each one corresponding to a different probability of observing a waterbird with a water background, and similarly with land birds.

In all settings, we use ResNet-50 [He et al., 2016], pretrained on ImageNet, and fine tuned for our specific task. All models are implemented in TensorFlow [Abadi et al., 2015]. We present the results from 20 simulations. In each simulation, we generate different train/test splits, and different bird-background combinations.

Methods. We compare the following methods in our experiments:

- 1. **wMMD-reg-T** is our main proposal, which minimizes equation 3, and applies the two-step cross validation process described in section 3.
- 2. **L2-reg-S** is the standard DNN trained to minimize the empirical risk. We introduce regularization by penalizing the L2-norm of the weights, picking the value of the penalty from 0.0 (no regularization), 0.0001, and 0.001 which is similar to values typically used for this setting [Sagawa et al., 2019, He et al., 2016].
- 3. wL2-reg-S: similar to L2-reg but also incorporates weighting using u as defined in 2.
- 4. **Rand-Aug-S**: a baseline that attempts to create a robust estimator by augmenting the data at training time using random flips and random rotations.

For L2-reg-S, wL2-reg-S and Rand-Aug-S cross-validation is done in the standard way, which simply picks the model that has the best performance on the held out validation set.

In the uncorrelated setting, we only present the unweighted variants of all the models, since the weights are roughly constant across data points in that setting.

Ablations. We also study several ablated variants of our approach:

- 1. **wMMD-reg-S** is similar to wMMD-reg-T, but uses standard cross-validation rather than our two-step cross-validation.
- 2. MMD-reg-T minimizes a variant of equation 3 but does not weight the loss or MMD by **u**. At validation-time, however, hyperparameters are picked using our two-step cross-validation approach with **u**—weighted estimates of the MMD and loss.
- 3. MMD-reg-S is similar to MMD-reg-T, but does standard cross-validation process.
- 4. **MMD-reg-uT** is similar to MMD-reg-T, but uses unweighted validation metric estimates during the two-step cross-validation procedure.

Results: Sampling from the optimal distribution. Figure 2 shows the results from the first setting, where the training data is sampled from the ideal, uncorrelated distribution P° , with $P^{\circ}(Y|V=1) = P^{\circ}(Y|V=0) = 0.5$. The x-axis shows P(Y=1|V=1) = P(Y=0|V=0) at test time, while the y-axis shows the corresponding mean AUROC, averaged over 20 simulations. The vertical dashed line shows the conditional probability at training time. We see that both variants of our proposed approach, with classical and two-step cross-validation outperform the L2-regularized model and the random augmentation model within the training distribution (i.e., at the dashed line) and when there is distribution shift. This conforms with our theory that suggests that even when the data are sampled from the optimal distribution, using a causally-motivated regularization scheme leads to more efficient models, which translates into better performance in finite samples. In addition, we see that all models are robust to distribution shift when trained on data from P° . This conforms with proposition 1, which states that under P° , optimal predictors are riskinvariant.

Results: Sampling from a correlated distribution. Figure 3 shows the results from the second setting, where the training data is sampled a correlated distribution with $P(Y = 1|V = 1) = P^{\circ}(Y = 0|V = 0) = 0.9$. The x, and y axes are similar to figure 2. Here we see that our main suggested approach (wMMD-reg-T) outperforms other models especially at high divergence from the training distribution. Out of all the non-MMD regularized baselines, the weighted L2-regularized model performs best. This suggests that minimizing the empirical risk on the \mathbf{u} -reweighted distribution contributes to model robustness.

Figure 4 shows an ablation study where we remove different components of our model to see how each contributes to improved performance. The largest increase in performance is attributable to weighting by \mathbf{u} at training time, since the two weighted variants outperform the two unweighted variants. Within those two groups, the two-step approach with weighted validation metrics outperforms the others, especially in terms of robustness to distribution shifts. This shows that when training models using the MMD-penalty, it is important to

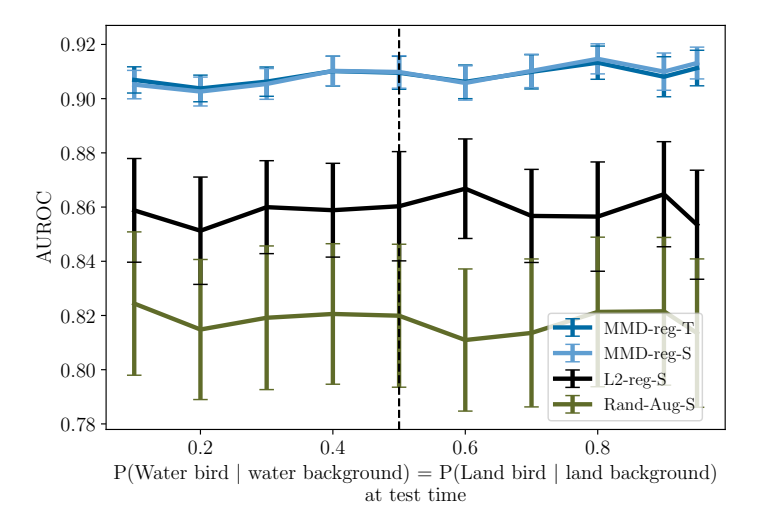


Figure 2: Training data sampled from P° , with $P^{\circ}(Y|V=1) = P^{\circ}(Y|V=0) = 0.5$. x-axis shows P(Y|V) at test time under different shifted distributions. y-axis shows AUROC on test data. Vertical dashed line shows training data. MMD-regularized models outperform baselines within, and outside the training distribution.

take into consideration that the MMD-penalty (unlike L2-norm regularization) also depends on the training data, and is prone to overfitting. The results also show that it is possible to improve the performance of models which are unweighted at training time by using our two step cross validation approach with weighted validation metrics, since MMD-reg-T slightly outperforms MMD-reg-S. Recall that MMD-reg-uT strictly enforces the MMD-penalty without addressing the fact that the training distribution has been sampled from a correlated distribution. We see that it gives a fairly robust model that has poor performance. This conforms with our findings stated in the appendix proposition A6, which implies that there will be a bias-robustness trade-off if the correlated sampling is not corrected.

6 Connections to existing work

Our work unifies several threads that have appeared in the ML literature.

Shortcut learning. The majority of work addressing shortcut learning relies on data augmentation: the practitioner defines a set of transformations (e.g., rotation, translation, cropping) that should not affect the main label, and adds the augmented examples to induce invariance to these transformations [Hendrycks et al., 2020, Yin et al., 2019, Lyle et al., 2020, Lopes et al., 2019, Cubuk et al., 2018]. One disadvantage of this approach is that it assumes the set of transformations is known a priori. If this set of transformations is misspecified, the desired robustness might not be achieved, as evidenced by the empirical performance of the random augmentation baseline presented in the experiments section. Our approach is different in that we do not claim to know these transformations. Instead, our approach leads to invariant models by leveraging the auxiliary labels to inform the relevant transformations the main label should be independent to.

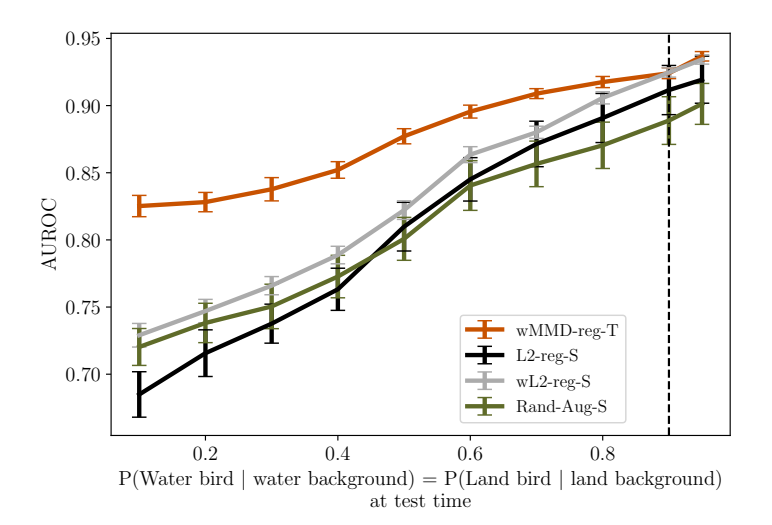


Figure 3: Training data sampled from P, with $P(Y=1|V=1)=P^{\circ}(Y=0|V=0)=0.9$. Vertical dashed line shows training data. x, y axes similar to figure 2. MMD-regularized models outperform baselines showing better robustness against distribution shifts at test time.

Shortcut learning can be viewed as a consequence of model underspecification [D'Amour et al., 2020]. Many of the issues related to underspecification have appeared in the ML literature within the context of overparameterization. For example, in Sagawa et al. [2020b] authors observe that overparameterization exacerbates the reliance on spurious correlations. Their suggested approach is somewhat similar to the reweighting baseline (wL2-reg-S) presented in the experiments section, which is outperformed by our model.

Invariant representations. Our work sheds light on properties of invariant representations, which are extensively studied in the fairness literature [Madras et al., 2018], causality literature [Shalit et al., 2017, Johansson et al., 2016], and domain shift literature [Tzeng et al., 2014, Long et al., 2015]. Specifically, our analysis (proposition 4) highlights how invariant representations regularize "redundant" dimensions. We also address one key question that has been discussed extensively recently: the question of whether there is a trade-off between invariance and accuracy, or stated differently: whether invariance leads to biased estimation [Zhang et al., 2019, Calders et al., 2009, Johansson et al., 2019, Dutta et al., 2020, Zhao and Gordon, 2019]. Propositions 3 shows that if the training data is sampled from the optimal distribution, then the MMD penalty does not lead to bias (i.e., there is no tradeoff). However, proposition A6 presented in the appendix shows that naively implementing the MMD penalty when the data is sampled from a biased distribution might lead to issues of bias. Our analysis suggests that if coupled with the correct sample reweighting the MMD penalty does not lead to bias.

More generally, while proposition 2 bears some similarity to statements presented in the domain adaptation literature [Long et al., 2015, Ben-David et al., 2007, 2010], our work is distinct in that we do not aim to generalize to a specific target domain. Instead, we aim to build models that generalize across a *family* of target domains. One consequence of

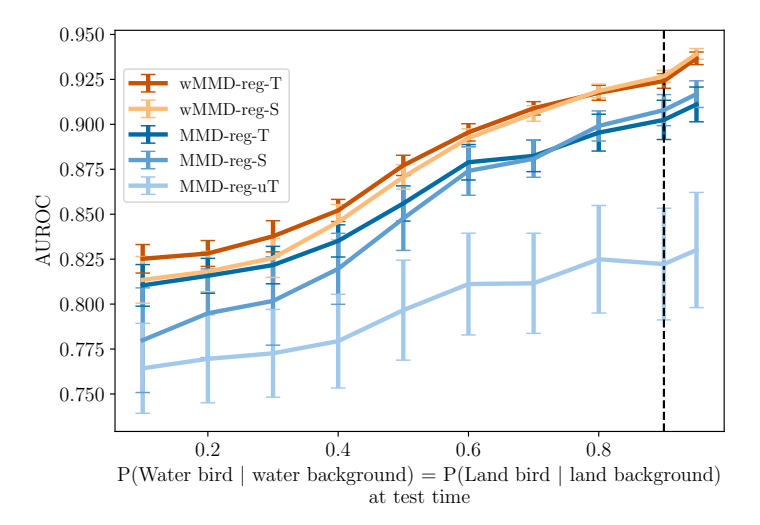


Figure 4: Training data sampled from P, with $P(Y = 1|V = 1) = P^{\circ}(Y = 0|V = 0) = 0.9$. x, y axes similar to figure 2.An ablation study to show how different components of our suggested approach (wMMD-reg-T) contribute to improved performance.

this distinction is that, unlike unsupervised domain adaptation, we do not require access to examples from a target domain.

Causally-motivated invariance. Our work is similar to Anchor regression [Rothenhäusler et al., 2018] in that we also view the question of invariance through the lens of causality. Our work is distinct in that we do not assume linear relationships between \mathbf{X}, Y , and the "anchor" variable V, and we are not limited to linear models. Arjovsky et al. [2019] propose an invariant risk minimization (IRM) approach that is inspired by ideas from causality. Unlike our approach, IRM does not explicitly penalize dependence on the redundant dimensions, and instead relies on the idea that, roughly speaking, the invariant risk minimizer should achieve the lowest error across datasets sampled from different target distributions P_t . As others (e.g., Guo et al. [2021], Rosenfeld et al. [2020]) have noted, when the family of functions is as flexible as DNNs, and without further assumptions on the training distribution, it is possible to find a predictor that achieves the objective of IRM but is not robust. Guo et al. [2021] attempted to address the limitations of IRM using an MMD penalty, however, they do not correct the estimates of the MMD for biased sampling and hence have the same limitations as the unweighted MMD models presented in the experiments.

7 Conclusion

We presented an approach to using auxiliary labels to build models that are invariant to distribution shifts. Guided by our theoretical insight, we suggested a causally-motivated regularization scheme to train robust, and accurate models. Using a well-known robustness benchmark, we show that our approach empirically outperforms others.

Societal impact. Our approach could be used in certain fairness applications where invariance to a sensitive label is favorable. We caution that even though our approach outperforms the baselines, it is imperfect in that it still exhibits some dependence on the features related to the sensitive (auxiliary) label as shown in figure 3. As with most learned models, human audits of the model's output are necessary in such high-stakes applications.

Limitations. Our approach requires a priori knowledge of the shortcut that might be exploited by the model. However, if the shortcut is unknown, practitioners can use interpretability methods to understand the main factors that the model relies on. If the interpretability analysis reveals that the model is relying on a shortcut, and if an auxiliary label that corresponds to that shortcut is available, our proposed approach can then be used. For example, in image classification, saliency maps can reveal the learned factors that influence the prediction the most [Simonyan et al., 2013]. In contexts other than image classification, other interpretability tools such as Shapley values are more appropriate [Lundberg and Lee, 2017, Wang et al., 2021].

References

Martín Abadi, Ashish Agarwal, Paul Barham, Eugene Brevdo, Zhifeng Chen, Craig Citro, Greg S. Corrado, Andy Davis, Jeffrey Dean, Matthieu Devin, Sanjay Ghemawat, Ian Goodfellow, Andrew Harp, Geoffrey Irving, Michael Isard, Yangqing Jia, Rafal Jozefowicz, Lukasz Kaiser, Manjunath Kudlur, Josh Levenberg, Dandelion Mané, Rajat Monga, Sherry Moore, Derek Murray, Chris Olah, Mike Schuster, Jonathon Shlens, Benoit Steiner, Ilya Sutskever, Kunal Talwar, Paul Tucker, Vincent Vanhoucke, Vijay Vasudevan, Fernanda Viégas, Oriol Vinyals, Pete Warden, Martin Wattenberg, Martin Wicke, Yuan Yu, and Xiaoqiang Zheng. TensorFlow: Large-scale machine learning on heterogeneous systems, 2015. URL https://www.tensorflow.org/. Software available from tensorflow.org.

Martin Arjovsky, Léon Bottou, Ishaan Gulrajani, and David Lopez-Paz. Invariant risk minimization. arXiv preprint arXiv:1907.02893, 2019.

Aharon Azulay and Yair Weiss. Why do deep convolutional networks generalize so poorly to small image transformations? arXiv preprint arXiv:1805.12177, 2018.

Sara Beery, Grant Van Horn, and Pietro Perona. Recognition in terra incognita. In *Proceedings of the European Conference on Computer Vision (ECCV)*, pages 456–473, 2018.

Shai Ben-David, John Blitzer, Koby Crammer, Fernando Pereira, et al. Analysis of representations for domain adaptation. *Advances in neural information processing systems*, 19:137, 2007.

Shai Ben-David, John Blitzer, Koby Crammer, Alex Kulesza, Fernando Pereira, and Jennifer Wortman Vaughan. A theory of learning from different domains. *Machine learning*, 79(1):151–175, 2010.

- Toon Calders, Faisal Kamiran, and Mykola Pechenizkiy. Building classifiers with independency constraints. In 2009 IEEE International Conference on Data Mining Workshops, pages 13–18. IEEE, 2009.
- Corinna Cortes, Yishay Mansour, and Mehryar Mohri. Learning bounds for importance weighting. In *Nips*, volume 10, pages 442–450. Citeseer, 2010.
- Ekin D Cubuk, Barret Zoph, Dandelion Mane, Vijay Vasudevan, and Quoc V Le. Autoaugment: Learning augmentation policies from data. arXiv preprint arXiv:1805.09501, 2018.
- Alexander D'Amour, Katherine Heller, Dan Moldovan, Ben Adlam, Babak Alipanahi, Alex Beutel, Christina Chen, Jonathan Deaton, Jacob Eisenstein, Matthew D Hoffman, et al. Underspecification presents challenges for credibility in modern machine learning. arXiv preprint arXiv:2011.03395, 2020.
- Sanghamitra Dutta, Dennis Wei, Hazar Yueksel, Pin-Yu Chen, Sijia Liu, and Kush Varshney. Is there a trade-off between fairness and accuracy? a perspective using mismatched hypothesis testing. In *International Conference on Machine Learning*, pages 2803–2813. PMLR, 2020.
- Dylan J Foster and Vasilis Syrgkanis. Orthogonal statistical learning. arXiv preprint arXiv:1901.09036, 2019.
- Robert Geirhos, Carlos RM Temme, Jonas Rauber, Heiko H Schütt, Matthias Bethge, and Felix A Wichmann. Generalisation in humans and deep neural networks. In *Advances in neural information processing systems*, pages 7538–7550, 2018.
- Robert Geirhos, Jörn-Henrik Jacobsen, Claudio Michaelis, Richard Zemel, Wieland Brendel, Matthias Bethge, and Felix A Wichmann. Shortcut learning in deep neural networks. arXiv preprint arXiv:2004.07780, 2020.
- Noah Golowich, Alexander Rakhlin, and Ohad Shamir. Size-independent sample complexity of neural networks. In *Conference On Learning Theory*, pages 297–299. PMLR, 2018.
- Arthur Gretton, Karsten M Borgwardt, Malte J Rasch, Bernhard Schölkopf, and Alexander Smola. A kernel two-sample test. *The Journal of Machine Learning Research*, 13(1):723–773, 2012.
- Ruocheng Guo, Pengchuan Zhang, Hao Liu, and Emre Kiciman. Out-of-distribution prediction with invariant risk minimization: The limitation and an effective fix. arXiv preprint arXiv:2101.07732, 2021.
- Kaiming He, Xiangyu Zhang, Shaoqing Ren, and Jian Sun. Deep residual learning for image recognition. In *Proceedings of the IEEE conference on computer vision and pattern recognition*, pages 770–778, 2016.
- Dan Hendrycks, Steven Basart, Norman Mu, Saurav Kadavath, Frank Wang, Evan Dorundo, Rahul Desai, Tyler Zhu, Samyak Parajuli, Mike Guo, et al. The many faces

- of robustness: A critical analysis of out-of-distribution generalization. arXiv preprint arXiv:2006.16241, 2020.
- Andrew Ilyas, Shibani Santurkar, Dimitris Tsipras, Logan Engstrom, Brandon Tran, and Aleksander Madry. Adversarial examples are not bugs, they are features. In *Advances in Neural Information Processing Systems*, pages 125–136, 2019.
- Fredrik Johansson, Uri Shalit, and David Sontag. Learning representations for counterfactual inference. In *International conference on machine learning*, pages 3020–3029. PMLR, 2016.
- Fredrik D Johansson, David Sontag, and Rajesh Ranganath. Support and invertibility in domain-invariant representations. In *The 22nd International Conference on Artificial Intelligence and Statistics*, pages 527–536. PMLR, 2019.
- Diederik P Kingma and Jimmy Ba. Adam: A method for stochastic optimization. In *ICLR*, 2015.
- Michel Ledoux. Isoperimetry and gaussian analysis. In *Lectures on probability theory and statistics*, pages 165–294. Springer, 1996.
- Francesco Locatello, Stefan Bauer, Mario Lucic, Gunnar Raetsch, Sylvain Gelly, Bernhard Schölkopf, and Olivier Bachem. Challenging common assumptions in the unsupervised learning of disentangled representations. In *international conference on machine learning*, pages 4114–4124, 2019.
- Mingsheng Long, Yue Cao, Jianmin Wang, and Michael Jordan. Learning transferable features with deep adaptation networks. In *International conference on machine learning*, pages 97–105. PMLR, 2015.
- Raphael Gontijo Lopes, Dong Yin, Ben Poole, Justin Gilmer, and Ekin D Cubuk. Improving robustness without sacrificing accuracy with patch gaussian augmentation. arXiv preprint arXiv:1906.02611, 2019.
- Scott Lundberg and Su-In Lee. A unified approach to interpreting model predictions. arXiv preprint arXiv:1705.07874, 2017.
- Clare Lyle, Mark van der Wilk, Marta Kwiatkowska, Yarin Gal, and Benjamin Bloem-Reddy. On the benefits of invariance in neural networks. arXiv preprint arXiv:2005.00178, 2020.
- David Madras, Elliot Creager, Toniann Pitassi, and Richard Zemel. Learning adversarially fair and transferable representations. arXiv preprint arXiv:1802.06309, 2018.
- Maggie Makar, Fredrik Johansson, John Guttag, and David Sontag. Estimation of bounds on potential outcomes for decision making. In *International Conference on Machine Learning*, pages 6661–6671. PMLR, 2020.
- Mehryar Mohri, Afshin Rostamizadeh, and Ameet Talwalkar. Foundations of machine learning. MIT press, 2018.

- Vaishnavh Nagarajan, Anders Andreassen, and Behnam Neyshabur. Understanding the failure modes of out-of-distribution generalization. arXiv preprint arXiv:2010.15775, 2020.
- Elan Rosenfeld, Pradeep Ravikumar, and Andrej Risteski. The risks of invariant risk minimization. arXiv preprint arXiv:2010.05761, 2020.
- Dominik Rothenhäusler, Nicolai Meinshausen, Peter Bühlmann, and Jonas Peters. Anchor regression: heterogeneous data meets causality. arXiv preprint arXiv:1801.06229, 2018.
- Shiori Sagawa, Pang Wei Koh, Tatsunori B Hashimoto, and Percy Liang. Distributionally robust neural networks for group shifts: On the importance of regularization for worst-case generalization. arXiv preprint arXiv:1911.08731, 2019.
- Shiori Sagawa, Aditi Raghunathan, Pang Wei Koh, and Percy Liang. An investigation of why overparameterization exacerbates spurious correlations. In Hal Daumé III and Aarti Singh, editors, *Proceedings of the 37th International Conference on Machine Learning*, volume 119 of *Proceedings of Machine Learning Research*, pages 8346–8356. PMLR, 13–18 Jul 2020a. URL http://proceedings.mlr.press/v119/sagawa20a.html.
- Shiori Sagawa, Aditi Raghunathan, Pang Wei Koh, and Percy Liang. An investigation of why overparameterization exacerbates spurious correlations. arXiv preprint arXiv:2005.04345, 2020b.
- Uri Shalit, Fredrik D Johansson, and David Sontag. Estimating individual treatment effect: generalization bounds and algorithms. In *Proceedings of the 34th International Conference on Machine Learning-Volume 70*, pages 3076–3085, 2017.
- Karen Simonyan, Andrea Vedaldi, and Andrew Zisserman. Deep inside convolutional networks: Visualising image classification models and saliency maps. arXiv preprint arXiv:1312.6034, 2013.
- Rohan Taori, Achal Dave, Vaishaal Shankar, Nicholas Carlini, Benjamin Recht, and Ludwig Schmidt. Measuring robustness to natural distribution shifts in image classification. *Advances in Neural Information Processing Systems*, 33, 2020.
- Eric Tzeng, Judy Hoffman, Ning Zhang, Kate Saenko, and Trevor Darrell. Deep domain confusion: Maximizing for domain invariance. arXiv preprint arXiv:1412.3474, 2014.
- Catherine Wah, Steve Branson, Peter Welinder, Pietro Perona, and Serge Belongie. The caltech-ucsd birds-200-2011 dataset. 2011.
- Jiaxuan Wang, Jenna Wiens, and Scott Lundberg. Shapley flow: A graph-based approach to interpreting model predictions. In *International Conference on Artificial Intelligence* and Statistics, pages 721–729. PMLR, 2021.
- Dong Yin, Raphael Gontijo Lopes, Jonathon Shlens, Ekin D Cubuk, and Justin Gilmer. A fourier perspective on model robustness in computer vision. arXiv preprint arXiv:1906.08988, 2019.

Hongyang Zhang, Yaodong Yu, Jiantao Jiao, Eric Xing, Laurent El Ghaoui, and Michael Jordan. Theoretically principled trade-off between robustness and accuracy. In *International Conference on Machine Learning*, pages 7472–7482. PMLR, 2019.

Han Zhao and Geoffrey J Gordon. Inherent tradeoffs in learning fair representations. arXiv preprint arXiv:1906.08386, 2019.

Bolei Zhou, Agata Lapedriza, Aditya Khosla, Aude Oliva, and Antonio Torralba. Places: A 10 million image database for scene recognition. *IEEE transactions on pattern analysis and machine intelligence*, 40(6):1452–1464, 2017.

A Proofs for section 2

To prove proposition 1, we first formally state the assumption of invertability mentioned in section 2. Specifically, the fact that \mathbf{X}^* is a function of \mathbf{X} only implies that \mathbf{X}^* is invertible, i.e. for all \mathbf{X} , \mathbf{X}^* can be exactly recovered from \mathbf{X} . We state that formally in the following assumption

Assumption A1. (Invertability) There exists some function e such that $\mathbf{X}^* = e(\mathbf{X})$ for all \mathbf{X} .

Proposition A1 (Restated proposition 1). Under P° , the Bayes optimal predictor is (i) only a function of \mathbf{X}^{*} , and (ii) an optimal risk-invariant predictor f_{rinv} with respect to \mathcal{P} .

Proof. Under P° , \mathbf{X}^{*} d-separates Y from \mathbf{X} , so $\mathbb{E}_{P^{\circ}}[Y \mid \mathbf{X}] = \mathbb{E}_{P^{\circ}}[Y \mid \mathbf{X}^{*}]$. Thus, the population risk minimizer is only a function of \mathbf{X}^{*} .

By the assumption A1, we have that $\mathbf{X}^* = e(\mathbf{X})$ and hence \mathbf{X}^* can be perfectly recovered from \mathbf{X} . This means that $\mathbb{E}_{P^{\circ}}[Y \mid \mathbf{X}^*]$ can be written as a function of \mathbf{X} , i.e., we can define $g(\mathbf{X}) = \mathbb{E}_{P^{\circ}}[Y \mid e(\mathbf{X})]$. Thus, the Bayes optimal classifier $f(\mathbf{X})$, which is a function of $\mathbb{E}_{P^{\circ}}[Y \mid \mathbf{X}] = \mathbb{E}_{P^{\circ}}[Y \mid e(\mathbf{X})]$, can be written (with some abuse of notation) as $f(\mathbf{X}^*)$ (that is, a function that only varies with the value of $\mathbf{X}^* = e(\mathbf{X})$).

Thus, the risk is also invariant. To see that note the following:

$$R^{\circ}(f) = \int_{\mathbf{X},Y} \ell(f(\mathbf{X}), Y) P^{\circ}(\mathbf{X} \mid \mathbf{X}^{*}, V) P^{\circ}(\mathbf{X}^{*} \mid Y) P^{\circ}(Y) P^{\circ}(V) dY d\mathbf{X}$$

$$= \int_{\mathbf{X}^{*}, Y} \ell(f(\mathbf{X}^{*}), Y) P^{\circ}(\mathbf{X}^{*} \mid Y) P^{\circ}(Y) dY d\mathbf{X}^{*}$$

$$= \int_{\mathbf{X}^{*}, Y} \ell(f(\mathbf{X}^{*}), Y) P(\mathbf{X}^{*} \mid Y) P(Y) dY d\mathbf{X}^{*}$$

$$= R_{P}(f),$$

for any $P \in \mathcal{P}$.

Because this classifier is optimal under P° , no other risk invariant classifier can obtain a lower risk across \mathcal{P} ; thus this classifier is an optimal risk invariant classifier.

B Proofs for section 3

We show that the reweighted risk is an unbiased estimator of the risk under P° , i.e., that

$$R_{Ps}^{\mathbf{u}}(f) = \mathbb{E}_{Ps}\left[\hat{R}_{Ps}^{\mathbf{u}}(f)\right] = R_{P^{\circ}}(f).$$

For any P_s , the **u**-weighted risk is equal to the risk under the corresponding unconfounded distribution P° . That is, $R_{Ps}^{\mathbf{u}} := \mathbb{E}_{Ps}[u(Y,V)\ell(f(\mathbf{X},Y))] = R_{P^{\circ}}$.

To see this, note that the conditional distribution $P_s(\mathbf{X} \mid Y, V)$ is invariant across the family \mathcal{P} defined in (1). Thus, the risk conditional on Y and V, $R_{Ps|y,v} := \mathbb{E}_{Ps}[\ell(f(\mathbf{X}), Y) \mid Y = y, V = v]$, does not change with P_s .

$$\begin{split} R_{Ps}^{\mathbf{u}}(f) &:= \mathbb{E}_{Ps}[u(Y,V)\ell(f(\mathbf{X},Y))] = \mathbb{E}_{Ps}[\mathbb{E}_{Ps}[u(Y,V)\ell(f(\mathbf{X},Y)) \mid Y = y, V = v]] \\ &= \sum_{y,v} P_s(Y = y, V = v)u(y,v)R_{P|y,v} = \sum_{y,v} P_s(Y = y)P_s(V = v)R_{Ps^{\circ}|y,v} \\ &= \mathbb{E}_{P^{\circ}}[\mathbb{E}_{P^{\circ}[R_{P^{\circ}|y,v}]}] = R_{P^{\circ}}. \end{split}$$

C Proofs for section 4.1

Lemma A1. For training data $\mathcal{D} = \{(\mathbf{x}_i, y_i, v_i)\}_{i=1}^n$, $\mathcal{D} \sim P^{\circ}$, and a corresponding learned $f = h(\phi(\mathbf{x}))$ with expected risk $R_{P^{\circ}}(f)$, suppose that y is ϕ -representable, i.e., that there exists $g(\phi(\mathbf{x})) = y$, and that $g(\phi)\ell(\phi) \in \Omega$. Then for all y:

$$P(Y=y)[R_{0y}^{\circ} - R_{1y}^{\circ}] \le \tau,$$

where $R_{vy}^{\circ} := \mathbb{E}_{\mathbf{x} \sim P^{\circ}}[\ell(f(\mathbf{x}), y) | V = v, Y = y]$

Proof. Without loss of generality, suppose that for y = 1,

$$P(Y = y)[R_{0y}^{\circ} - R_{1y}^{\circ}] = \tau_1 > \tau.$$

Then due to the fact that MMD $\leq \tau$, and by assumption that $\ell \in \Omega$

$$P(Y = 0)[R_{00}^{\circ} - R_{10}^{\circ}] \le \tau - \tau_1$$

$$P(Y = 0)[R_{00}^{\circ} - R_{10}^{\circ}] < 0$$

$$R_{00}^{\circ} - R_{10}^{\circ} < 0.$$

Using the shorthand $R_{\Delta 0}^{\circ} := R_{00} - R_{10}$, the above inequality implies that $-R_{\Delta 0}^{\circ} > 0$.

Let $\dot{\ell}(\phi) = (2g(\phi) - 1) \cdot \ell(\phi)$, and $\dot{R}^{\circ} := \mathbb{E}[\dot{\ell}(\phi)]$. By assumption, we have that $\dot{\ell}$ is also $\in \Omega$. However,

$$\begin{split} \text{MMD}(\mathring{\ell}, P_{\phi_0}, P_{\phi_1}) &= P(Y = 0) [\mathring{R}_{00}^{\circ} - \mathring{R}_{10}^{\circ}] + P(Y = 1) [\mathring{R}_{01}^{\circ} - \mathring{R}_{11}^{\circ}] \\ &= P(Y = 0) [-(R_{00}^{\circ} - R_{10}^{\circ})] + P(Y = 1) [R_{01}^{\circ} - R_{11}^{\circ}] \\ &= P(Y = 0) [-R_{\Delta 0}^{\circ}] + \tau_1 > \tau. \end{split}$$

This contradicts the MMD condition; that for all functions in Ω , MMD $\leq \tau$

Proposition A2 (Restated proposition 2). Suppose that $f = h(\phi(\mathbf{X}))$ is a predictor that satisfies $\mathrm{MMD}(P_{\phi_0}^{\circ}, P_{\phi_1}^{\circ}) \leq \tau$. Suppose that y is ϕ -representable, i.e., that there exists $g(\phi(\mathbf{x})) = y$, and that $g(\phi)\ell(\phi) \in \Omega$. Then

$$R_{Pt}(f) < R_{P^{\circ}}(f) + 2\tau.$$

Proof. We will use $P_{v|y}(v) := P(V = v|Y = v)$, $P_y(y) = P(Y = y)$, $P_v(v) = P(V = v)$, and R_{vv}° as defined in lemma A1.

Note that

$$R_{P^{\circ}} = \sum_{y} P_{y}^{\circ}(y) \left[P_{v|y}^{\circ}(0) R_{0,y}^{\circ} + P_{v|y}^{\circ}(1) R_{1,y}^{\circ} \right]$$
$$= \sum_{y} P_{y}(y) \left[P_{v}^{\circ}(0) R_{0,y}^{\circ} + P_{v}^{\circ}(1) R_{1,y}^{\circ} \right].$$

And:

$$R_P = \sum_{y} P_y(y) \left[P_{v|y}(0) R_{0,y}^{\circ} + P_{v|y}(1) R_{1,y}^{\circ} \right].$$

Taking the difference between the two:

$$R_{P} - R_{P^{\circ}} = \sum_{y} P_{y}(y) \left[\left(P_{v|y}(0) - P_{v}^{\circ}(0) \right) R_{0,y}^{\circ} + \left(P_{v|y}(1) - P_{v}^{\circ}(1) \right) R_{1,y}^{\circ} \right]$$

$$= \sum_{y} P_{y}(y) \left[\left(P_{v|y}(0) - P_{v}^{\circ}(0) \right) R_{0,y}^{\circ} + \left(\left(1 - P_{v|y}(0) \right) - \left(1 - P_{v}^{\circ}(0) \right) \right) R_{1,y}^{\circ} \right]$$

$$= \sum_{y} P_{y}(y) \left[\left(P_{v|y}(0) - P_{v}^{\circ}(0) \right) R_{0,y}^{\circ} - \left(P_{v|y}(0) - P_{v}^{\circ}(0) \right) R_{1,y}^{\circ} \right]$$

$$= \sum_{y} P_{y}(y) \left[\beta_{y} R_{0,y}^{\circ} - \beta_{y} R_{1,y}^{\circ} \right]$$

$$= \sum_{y} \beta_{y} P_{y}(y) \left[R_{0,y}^{\circ} - R_{1,y}^{\circ} \right]$$

$$\leq \sum_{y} \beta_{y} \tau$$

$$= \beta \cdot \tau$$

where in the fourth equality, we use the shorthand $\beta_y := P_{v|y}(0) - P_v^{\circ}(0)$, and $-1 < \beta_y < 1$. The first inequality follows from lemma A1, and the last equality follows from setting $\beta = \sum_y \beta_y$. Since $\beta \leq 2$, this completes our proof.

D Proofs for section 4.2

Proposition A3. (Restated proposition 3) For $\mathcal{D} \sim P^{\circ}$, and for any for any \mathcal{F}_{L_2} such that $f_{rinv} \in \mathcal{F}_{L_2}$, there exists a $\mathcal{F}_{\text{MMD},L_2} \subseteq \mathcal{F}_{L_2}$ such that $f_{rinv} \in \mathcal{F}_{\text{MMD},L_2}$. And the smallest $\mathcal{F}_{\text{MMD},L_2}$ such that $f_{rinv} \in \mathcal{F}_{\text{MMD},L_2}$ has MMD = 0.

Proof. We prove the existence of a subset, $\mathcal{F}_{\text{MMD},L_2} \subset \mathcal{F}_{L_2}$ by giving an example of such a subset. Consider

$$\mathcal{F}_{L_2,\text{MMD}} = \{ f : \mathbf{x} \mapsto \sigma(\mathbf{w}^{\top} \mathbf{x}), \|\mathbf{w}\|_2 \le A, \text{ MMD}(P_{\phi_0}^{\circ}, P_{\phi_1}^{\circ}) = 0 \},$$

Clearly, $\mathcal{F}_{\text{MMD},L_2} \subset \mathcal{F}_{L_2}$. We will now show that any $f_{\text{rinv}} \in \mathcal{F}_{L_2}$ is also $\in \mathcal{F}_{\text{MMD},L_2}$.

By the definition of f_{rinv} , any $f_{\text{rinv}} \in \mathcal{F}_{L_2}$ must satisfy $f_{\text{rinv}}(\mathbf{x}) \perp v$. Then $T_1(f_{\text{rinv}}(\mathbf{x})) \perp T_2(v)$ for any transformations T_1, T_2 . Taking T_1 to be the inverse of the sigmoid function, σ^{-1} , and T_2 to be the identity transformation, we get that $\sigma^{-1}(f_{\text{rinv}}(\mathbf{x})) = \sigma^{-1}(\sigma(\mathbf{w}^{\top}\mathbf{x})) = \mathbf{w}^{\top}\mathbf{x} \perp v$. This implies that $p(\mathbf{w}^{\top}\mathbf{x}|v=0) = p(\mathbf{w}^{\top}\mathbf{x}|v=1)$, which in turn implies that $MMD(P_{\phi_0}^{\circ}, P_{\phi_1}^{\circ}) = 0$, where $\phi(\mathbf{x}) = \mathbf{w}^{\top}\mathbf{x}$.

Proposition A4. (Restated proposition 4). Let $f(\mathbf{x}) = \sigma(\phi(\mathbf{x})) = \sigma(\mathbf{w}^{\top}\mathbf{x})$ be a function contained in $\mathcal{F}_{L_2,\text{MMD}}$. Then,

$$\|\mathbf{w}_{\perp}\| \le \frac{\tau}{\|\Delta\|}.\tag{8}$$

Proof. Note that τ must be greater than 0. If not, let ω' be the function that achieves the max difference $\tau' < 0$. Then we can define $\omega'' = -\omega'$, which achieves $\tau'' = -\tau' > 0$, which is a contradiction. This means that for all $\omega \in \Omega$,

$$\tau \ge |\mathbb{E}[\omega(\mathbf{x}_i) \mid v_i = 0] - \mathbb{E}[\omega(\mathbf{x}_i) \mid v_i = 1]|$$

Taking $\omega(\mathbf{x}) = \mathbf{w}^{\top} \mathbf{x}$,

$$\tau \ge \left| \mathbb{E}[\mathbf{w}^{\top} \mathbf{x}_i \mid v_i = 0] - \mathbb{E}[\mathbf{w}^{\top} \mathbf{x}_i \mid v_i = 1] \right| = \left| \mathbf{w}^{\top} \Delta \right|.$$

Note that $\|\mathbf{w}_{\perp}\| = \frac{|\mathbf{w}^{\top}\Delta|}{\|\Delta\|}$, which completes our proof.

Proposition A5. (Restated Proposition 5). Let $\mathbf{x}_{\perp} := \Pi \mathbf{x}$, $\mathbf{x}_{\parallel} := (I - \Pi) \mathbf{x}$. For training data $\mathcal{D} = \{(\mathbf{x}_i, y_i, v_i)\}_{i=1}^n$, $\mathcal{D} \sim P^{\circ}$, $\sup_{\mathbf{x}_{\perp}} \|\mathbf{x}_{\perp}\|_2 \leq B_{\perp}$, $\sup_{\mathbf{x}_{\parallel}} \|\mathbf{x}_{\parallel}\|_2 \leq B_{\parallel}$,

$$\Re(\mathcal{F}_{L_2}) \le \frac{A\sqrt{B_{\parallel}^2 + B_{\perp}^2}}{\sqrt{n}},$$

and

$$\Re(\mathcal{F}_{\mathrm{MMD},L_2}) \leq \frac{A \cdot B_{\parallel} + \tau \frac{B_{\perp}}{\|\Delta\|}}{\sqrt{n}}.$$

Proof. First, we derive the bound on $\Re(\mathcal{F}_{L_2})$

$$\mathfrak{R}(\mathcal{F}_{L_2}) = \mathbb{E}_{\mathcal{D}} \mathbb{E}_{\epsilon} \left[\sup_{\mathbf{w}: ||\mathbf{w}||_2 \le A} \frac{1}{n} \sum_{i} \epsilon_i \mathbf{w}^{\top} \mathbf{x}_i \right]$$
$$= \mathbb{E}_{\mathcal{D}} \mathbb{E}_{\epsilon} \left[\sup_{\mathbf{w}: ||\mathbf{w}||_2 \le A} \frac{1}{n} \sum_{i} \epsilon_i \mathbf{w}^{\top} (\mathbf{x}_{\perp i} + \mathbf{x}_{\parallel i}) \right]$$

Following the usual derivations (e.g., see Mohri et al. [2018]), we get the desired result for $\mathfrak{R}(\mathcal{F}_{L_2})$. Next, we derive the bound on $\mathfrak{R}(\mathcal{F}_{\mathrm{MMD},L_2})$.

$$\mathfrak{R}(\mathcal{F}_{\mathrm{MMD},L_{2}}) = \mathbb{E}_{\mathcal{D}} \mathbb{E}_{\epsilon} \left[\sup_{\mathbf{w}:\|\mathbf{w}\|_{2} \leq A} \frac{1}{n} \sum_{i} \epsilon_{i} \mathbf{w}^{\top} \mathbf{x}_{i} \right]
= \mathbb{E}_{\mathcal{D}} \mathbb{E}_{\epsilon} \left[\sup_{\mathbf{w}:\|\mathbf{w}\|_{2} \leq A} \frac{1}{n} \sum_{i} \epsilon_{i} \left(\Pi \mathbf{w}^{\top} \mathbf{x}_{i} + (1 - \Pi) \mathbf{w}^{\top} \mathbf{x}_{i} \right) \right]
\leq \mathbb{E}_{\mathcal{D}} \mathbb{E}_{\epsilon} \left[\sup_{\mathbf{w}_{\parallel}:\|\mathbf{w}_{\parallel}\|_{2} \leq A} \frac{1}{n} \sum_{i} \epsilon_{i} \mathbf{w}_{\perp}^{\top} \mathbf{x}_{\perp i} + \epsilon_{i} \mathbf{w}_{\parallel}^{\top} \mathbf{x}_{\parallel i} \right]
\leq \mathbb{E}_{\mathcal{D}} \mathbb{E}_{\epsilon} \left[\sup_{\mathbf{w}_{\perp}:\|\mathbf{w}_{\perp}\|_{2} \leq A} \frac{1}{n} \sum_{i} \epsilon_{i} \mathbf{w}_{\perp}^{\top} \mathbf{x}_{\perp i} \right] + \mathbb{E}_{\mathcal{D}} \mathbb{E}_{\epsilon} \left[\sup_{\mathbf{w}_{\parallel}:\|\mathbf{w}_{\parallel}\|_{2} \leq A} \frac{1}{n} \sum_{i} \epsilon_{i} \mathbf{w}_{\parallel}^{\top} \mathbf{x}_{\parallel i} \right],$$

where the last inequality follows by the subadditivity of the supremum. Again, following the usual derivations (e.g., see Mohri et al. [2018]), we get the required result for $\Re(\mathcal{F}_{\text{MMD},L_2})$

In the following proposition we show that when sampling from a biased distribution, the smallest τ' that does not introduce bias is greater than 0.

Proposition A6. Let $\mathcal{F}'_{L_2,\text{MMD}} := \{ f : \mathbf{x} \mapsto \sigma(\mathbf{w}^\top \mathbf{x}), \|\mathbf{w}\|_2 \leq A, \text{ MMD}(P_{\phi_0}, P_{\phi_1}) \leq \tau' \}$ be the smallest function class that contains f_{rinv} . Then $\tau' = c \cdot A$ for some c > 0, and the corresponding upper bound on the Rademacher complexity of $\mathcal{F}'_{\text{MMD},L_2}$ is

$$\Re(\mathcal{F}'_{\mathrm{MMD},L_2}) \le \frac{A \cdot B_{\parallel} + c \cdot A \frac{B_{\perp}}{\|\Delta\|}}{\sqrt{n}}.$$

Proof. By proposition 3, we have that the smallest MMD regularized function class that contains f_{rinv} when $\mathcal{D} \sim P^{\circ}$ has MMD = 0. And by proposition 4 we have in that function class $\|\mathbf{w}_{\perp}\| = 0$, i.e., \mathbf{w}_{\perp} is the 0 vector.

$$\tau' \geq \left\| \mathbb{E}[\mathbf{w}^{\top} \mathbf{x}_{i} \mid v_{i} = 0] - \mathbb{E}[\mathbf{w}^{\top} \mathbf{x}_{i} \mid v_{i} = 1] \right\|$$

$$= \left\| \mathbb{E}[\mathbf{w}_{\perp}^{\top} \mathbf{x}_{\perp i} + \mathbf{w}_{\parallel}^{\top} \mathbf{x}_{\parallel i} \mid v_{i} = 0] - \mathbb{E}[\mathbf{w}_{\perp}^{\top} \mathbf{x}_{\perp i} + \mathbf{w}_{\parallel}^{\top} \mathbf{x}_{\parallel i} \mid v_{i} = 1] \right\|$$

$$= \left\| \mathbb{E}[\mathbf{w}_{\parallel}^{\top} \mathbf{x}_{\parallel i} \mid v_{i} = 0] - \mathbb{E}[\mathbf{w}_{\parallel}^{\top} \mathbf{x}_{\parallel, i} \mid v_{i} = 1] \right\|$$

$$= \left\| \mathbf{w}_{\parallel} (\mathbb{E}[\mathbf{x}_{\parallel i} \mid v_{i} = 0] - \mathbb{E}[\mathbf{x}_{\parallel, i} \mid v_{i} = 1]) \right\|$$

$$= \left\| \mathbf{w}_{\parallel} (1 - \Pi) (\mathbb{E}[\mathbf{x}_{i} \mid v_{i} = 0] - \mathbb{E}[\mathbf{x}_{i} \mid v_{i} = 1]) \right\|$$

$$= \|\mathbf{w}_{\parallel} \| \| (1 - \Pi) (\mathbb{E}[\mathbf{x}_{i} \mid v_{i} = 0] - \mathbb{E}[\mathbf{x}_{i} \mid v_{i} = 1]) \|$$

$$= A \| (1 - \Pi) \Delta_{P} \|,$$

where the fifth equality holds because the two vectors are scalar multiples of the same vector (they are both projections onto the vector orthogonal to Δ) so Cauchy-Schwartz holds with equality. Also note that $\|(1-\Pi)\Delta_P\|=0$ if and only if $\Delta_P=\Delta$, i.e., $P=P^\circ$. So $\|(1-\Pi)\Delta_P\|>0$.

The upper bound on the Rademacher complexity follows immediately by plugging the upper bound on τ' into $\mathfrak{R}(\mathcal{F}_{\mathrm{MMD},L_2})$ obtained in proposition 5.

Notes on proposition A6

1. One important implication of proposition A6 is that naively implementing the MMD penalty when the data are sampled from some $P_s \neq P^{\circ}$ will lead to a bias-invariance tradeoff. For any $\tau' < c \cdot A$, invariance comes at the cost of bias. To understand why, note that when $\tau' < c \cdot A$, the optimal function does not exist in the candidate function class. Recall that when sampling from P° , we could allow τ to go to zero without introducing bias.

2. Comparing the upper bound on $\mathfrak{R}(\mathcal{F}_{\mathrm{MMD},L_2})$ in proposition 5 to $\mathfrak{R}(\mathcal{F}'_{\mathrm{MMD},L_2})$ in proposition A6 shows that the statistical complexity increases when sampling from $P_s \neq P^{\circ}$. Consequently, the generalization error is higher (i.e., less favorable) when sampling from a non-ideal, correlated distribution.

D.1 Full generalization error statements

We start with the simpler case, where $\mathcal{D} \sim P^{\circ}$.

Proposition A7. For a dataset $\mathcal{D} \sim P^{\circ}$, and loss bounded above by M > 0, the finite-sample gap

$$R_{P^{\circ}}(f) - \hat{R}_{P^{\circ}}(f) \le \frac{A \cdot B_{\parallel} + \tau \frac{B_{\perp}}{\|\Delta\|}}{\sqrt{n}} + M \sqrt{\frac{\log \frac{1}{\delta}}{2n}},$$

Proof. The proof is a straightforward application of theorem 11.3 in Mohri et al. [2018]. The result can be immediately acquired by substituting μ in theorem 11.3 with 1 (since the logistic loss is 1-Lipschitz), and $\mathfrak{R}_m(\mathcal{H})$ with $\mathfrak{R}(\mathcal{F}_{\text{MMD},L_2})$ from proposition 5.

To get a similar statement for the case where $\mathcal{D} \sim P_s \neq P^{\circ}$, and reweighting is needed, we need to apply the techniques for estimating the generalization error of reweighted estimators presented in Cortes et al. [2010]. To apply the Cortes results, we need to construct a discretization or a covering of $\mathcal{F}_{L_2,\text{MMD}}$, defined next.

Definition A1. Given any function class \mathcal{F} , a metric D on the elements of \mathcal{F} , and $\varepsilon > 0$, we define a covering number $\mathcal{N}(\mathcal{F}, D, \varepsilon)$ as the minimal number m of functions $f_1, f_2, \ldots, f_m \in \mathcal{F}$, such that for all $f \in \mathcal{F}$, $\min_{i=1,\ldots,m} D(f_i, f) \leq \varepsilon$, with

$$D(f, f') = \sqrt{\frac{1}{n} \sum_{i} (f(\mathbf{x}_i) - f'(\mathbf{x}_i))^2}.$$

Our statement also makes use of Gaussian complexities, defined next.

Definition A2. For a function family \mathcal{F} , the empirical Gaussian complexity is defined as:

$$\mathfrak{G}(\mathcal{F}) = \mathbb{E}_{\mathcal{D}} \mathbb{E}_{\eta} \left[\sup_{f \in \mathcal{F}} \eta_i f(\mathbf{x}_i)
ight]$$

We are now ready to present the metric entropy of the discretized hypothesis space in this next lemma.

Lemma A2. Let $\mathbf{x}_{\perp} := \Pi \mathbf{x}$, $\mathbf{x}_{\parallel} := (I - \Pi) \mathbf{x}$, $\sup_{\mathbf{x}_{\perp}} \|\mathbf{x}_{\perp}\|_{2} \leq B_{\perp}$, $\sup_{\mathbf{x}_{\parallel}} \|\mathbf{x}_{\parallel}\|_{2} \leq B_{\parallel}$, D, ε as is defined in A1. For $\varepsilon, c', c'' > 0$:

$$\log(\mathcal{N}(\mathcal{F}_{L_2,\text{MMD}}, D, \varepsilon)) \le c'' \left(\frac{c' \sqrt{\log(n)} \cdot \left(A \cdot B_{\parallel} + \tau \frac{B_{\perp}}{\|\Delta\|} \right)}{\varepsilon} \right)^2$$

Proof. We construct our argument relying on Sudakov's minoration, and the bound between Gaussian and Rademacher complexities. Specifically, by Ledoux [1996], for some c' > 0:

$$\mathfrak{G}_{m}(\mathcal{F}_{L_{2},\text{MMD}}) \leq c' \sqrt{\log(n)} \cdot \mathfrak{R}(\mathcal{F}_{L_{2},\text{MMD}})$$
$$\leq c' \sqrt{\log(n)} \cdot \frac{A \cdot B_{\parallel} + \tau \frac{B_{\perp}}{\|\Delta\|}}{\sqrt{n}},$$

where the last inequality follows from plugging in the results from proposition 5. By Sudakov's minoration (see Ledoux [1996] theorem 3.18), for some universal constant c'' > 0,

$$\log(\mathcal{N}(\mathcal{F}_{L_2,\text{MMD}}, D, \varepsilon)) \leq c'' \left(\frac{\sqrt{n} \cdot \mathfrak{G}_m(\mathcal{F}_{L_2,\text{MMD}})}{\varepsilon}\right)^2$$
$$\leq c'' \left(\frac{c'\sqrt{\log(n)} \cdot \left(A \cdot B_{\parallel} + \tau \frac{B_{\perp}}{\|\Delta\|}\right)}{\varepsilon}\right)^2$$

Finally, to use the Cortes et al. [2010] results, we need bounded divergence between the source and the target distribution. Recall that we are trying to bound the finite-sample gap, so the source distribution is P_s , and the target distribution is P° . We can bound this

divergence because of the overlap assumption stated in section 2. As a consequence of the overlap assumption, we have that:

$$\sup u(y,v) = \sup \frac{P^{\circ}(Y \mid V)}{P_s(Y \mid V)} = 2^{\Xi_{\infty}(P^{\circ}||P_s)} = C_{Ps}, \tag{9}$$

where $\Xi_k(p||q)$ is the kth-order Rényi divergence, and the second equality follows by applying the Bayes rule, and the definition of the Rényi divergence. It will be convenient to denote $2^{\Xi_k(p||q)}$ by $\Lambda_k(p||q)$. Since $2^{\Xi_k-1(P^\circ||P_s)} < 2^{\Xi_k(P^\circ||P_s)}$, we have $\Lambda_2(P^\circ||P_s) < C_{P_s}$. Following similar work (e.g., Makar et al. [2020]), we will assume that the weights \mathbf{u} are known, or can be perfectly estimated from the data. In other words, we do not consider estimation error that might arise because of poor estimation of \mathbf{u} . Work by Foster and Syrgkanis [2019] has shown that under mild assumptions, the error due to estimation of \mathbf{u} from finite samples

only results in a fourth order dependence in the final classifier, and hence does not greatly affect our derived generalization bounds.

With that, we are ready to state the finite-gap bound when $P_s \neq P^{\circ}$, and reweighting is used.

Proposition A8. For $\mathcal{D} \sim P$, with $P \in \mathcal{P}$, and \mathbf{u} as defined in equation 2, C_P as defined in equation 9,

$$R_{P^{\circ}}(f) - \hat{R}_{P}^{\mathbf{u}}(f) \leq \frac{2C_{P}(\kappa(\mathcal{F}_{\mathrm{MMD},L_{2}}) + \log\frac{1}{\delta})}{2n} + \sqrt{\frac{\Lambda(P^{\circ}||P) \cdot (\kappa(\mathcal{F}) + \log\frac{1}{\delta})}{n}},$$

where

$$\kappa(\mathcal{F}_{\mathrm{MMD},L_2}) = c'' \left(\frac{c' \sqrt{\log(n)} \cdot \left(A \cdot B_{\parallel} + \tau \frac{B_{\perp}}{\|\Delta\|} \right)}{\varepsilon} \right)^2$$

Proof. Using the bound on the metric entropy derived in lemma A2, the proof becomes a direct application of Theorem 2 in Cortes et al. [2010]. \Box

E Experiments

E.1 Example images

Figure 5 shows examples of the generated images.

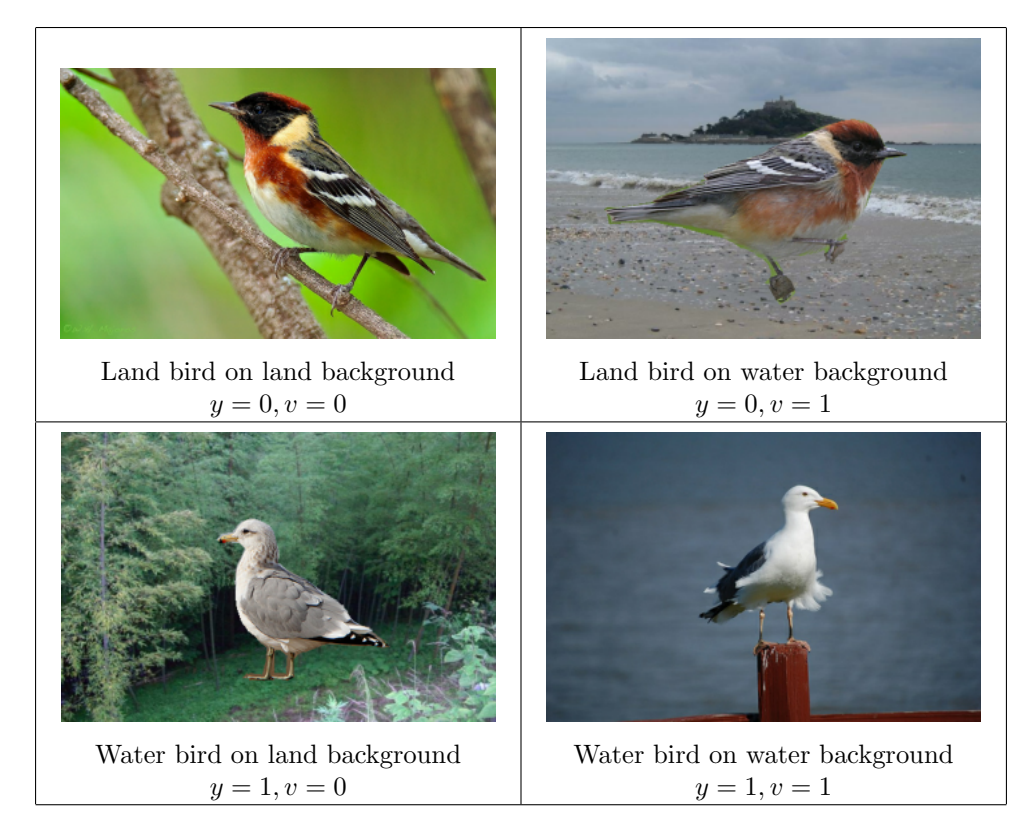


Figure 5: Examples of the generated images of water, and land birds on water, and land backgrounds

E.2 Hyperparameter setting

We train all models using Adam Kingma and Ba [2015], with learning rate = 0.001, $\beta_1 = 0.9$, $\beta_2 = 0.999$. We train all models for 200 epochs. For L_2 regularized models, we cross-validate the L_2 penalty parameter from the following values [0.0 (no regularization), 0.001, 0.0001]. For the MMD regularized models, we pick the optimal MMD penalty parameter, α from [1e³, 1e⁵, 1e⁷]. We also pick the best RBF kernel bandwidth from [1e1, 1e2, 1e3].

For our two-step cross-validation, we determine that a model has an MMD that is statistically insignificantly different from 0 by using a standard T-test. Specifically, we compare the mean MMD across 5 folds of validation data to 0. If the P-value of that T-test is greater than 0.05, we say that the model has an MMD that is statistically insignificantly different from 0.

E.3 Noisy background

We found that the original background images frequently contain landscapes that are difficult to distinguish (e.g., water backgrounds with very small water bodies that mostly reflect the surrounding trees). To address that, we pick 300 "clean" images for each of the land and water backgrounds. Using those clean images, we generate 10,000 land backgrounds, and 9,000 water backgrounds by applying random transformations (rotation, zoom, darkening/brightening) to the selected images. Figure 6 shows examples of the excluded backgrounds. To protect the privacy of the individuals in the pictures, their faces have been blurred.

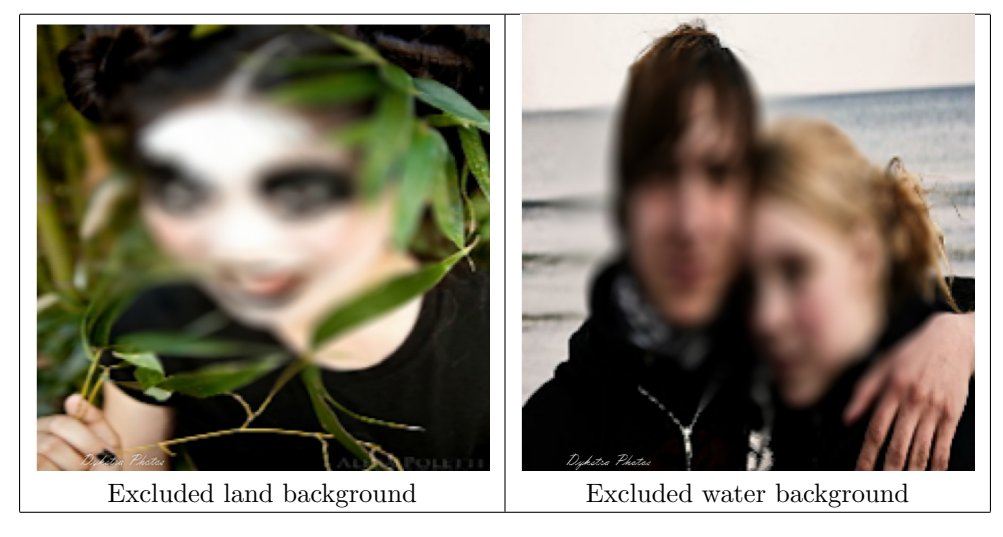


Figure 6: Examples of excluded noisy backgrounds. Pictures extracted from the Places dataset Zhou et al. [2017]. Blurring is added to preserve privacy.

Here we present the results using the full (noisy) background images. Results from the main analysis largely hold, with the exception of the results from the training setting where the data are sampled from the ideal distribution P° . Because the backgrounds are noisy, we see an overall higher variance in performance, so the models perform equally well with no clear "winner".

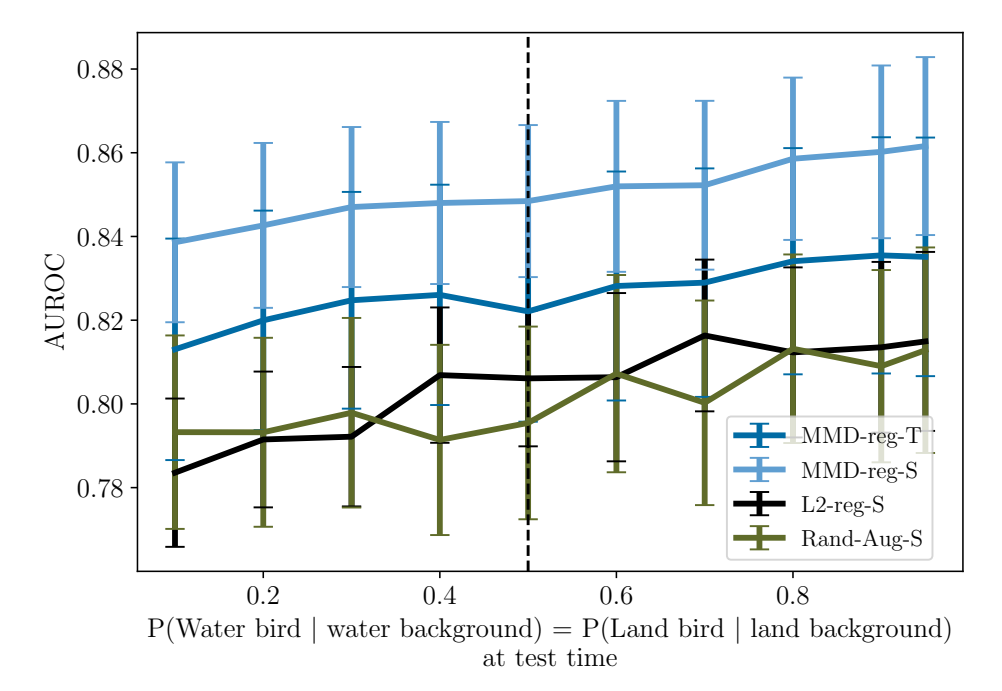


Figure 7: Training data sampled from P° , with $P^{\circ}(Y|V=1) = P^{\circ}(Y|V=0) = 0.5$ and backgrounds are sampled from a noisy set of images. x-axis shows P(Y|V) at test time under different shifted distributions. y-axis shows AUROC on test data. Vertical dashed line shows training data. MMD-regularized models outperform baselines within, and outside the training distribution.

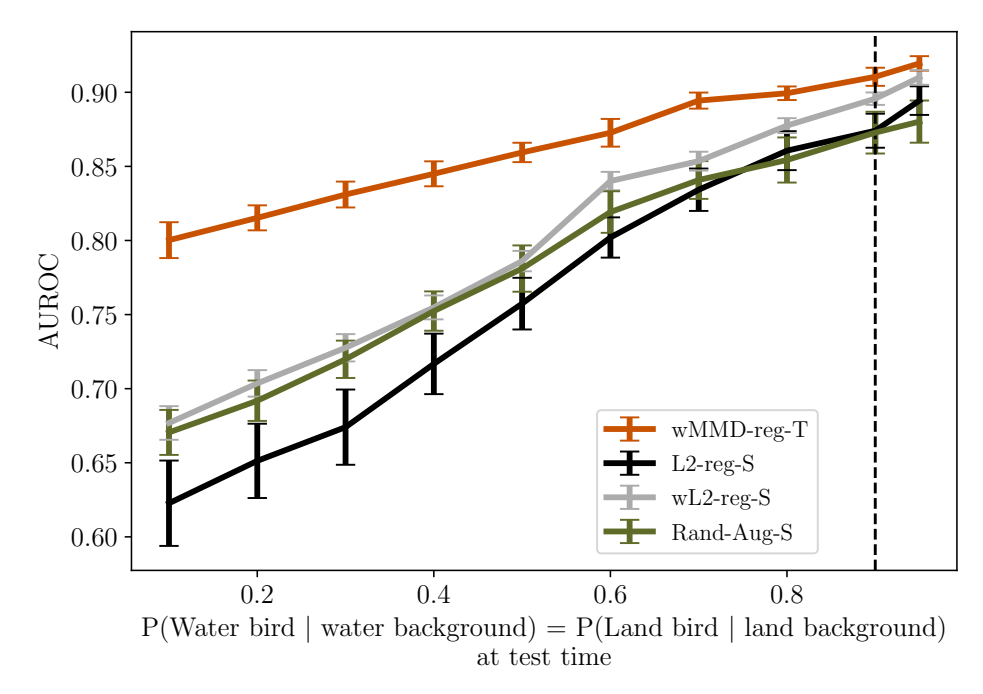


Figure 8: Training data sampled from P, with $P(Y=1|V=1)=P^{\circ}(Y=0|V=0)=0.9$, and backgrounds are sampled from a noisy set of images. Vertical dashed line shows training data. x, y axes similar to figure 7. MMD-regularized models outperform baselines showing better robustness against distribution shifts at test time.

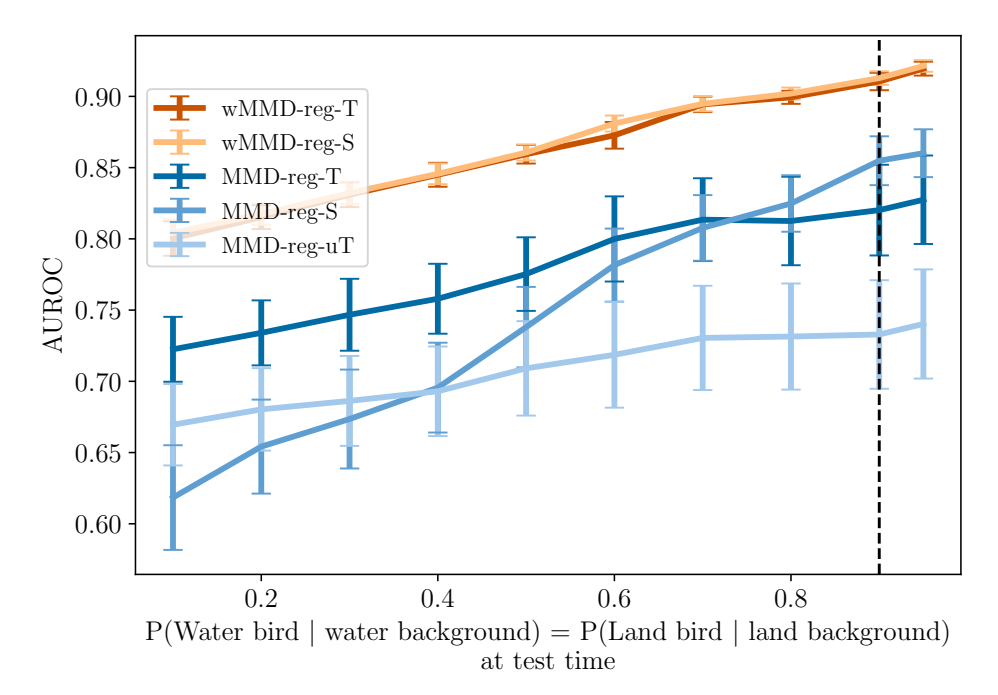


Figure 9: Training data sampled from P, with $P(Y=1|V=1)=P^{\circ}(Y=0|V=0)=0.9$. x, and backgrounds are sampled from a noisy set of images. y axes similar to fig 7. An ablation study to show how different components of our suggested approach (wMMD-reg-T) contribute to improved performance.